Characterisation of a novel mouse liver aldo-keto reductase AKR7A5

Alison Hinshelwood[a,b], Gail McGarvie[b], Elizabeth Ellis[a,c,*]

[a] *Department of Pharmaceutical Sciences, University of Strathclyde, 204 George Street, Glasgow G1 1XW, UK*
[b] *School of Science and Technology, Bell College, Almada Street, Hamilton, Lanarkshire ML3 OJB, UK*
[c] *Department of Bioscience, University of Strathclyde, 204 George Street, Glasgow G1 1XW, UK*

Revised 12 June 2002; accepted 12 June 2002

First published online 25 June 2002

Edited by Stuart Ferguson

Abstract We have characterised a novel aldo-keto reductase (AKR7A5) from mouse liver that is 78% identical to rat aflatoxin dialdehyde reductase AKR7A1 and 89% identical to human succinic semialdehyde (SSA) reductase AKR7A2. AKR7A5 can reduce 2-carboxybenzaldehyde (2-CBA) and SSA as well as a range of aldehyde and diketone substrates. Western blots show that it is expressed in liver, kidney, testis and brain, and at lower levels in skeletal muscle, spleen heart and lung. The protein is not inducible in the liver by dietary ethoxyquin. Immunodepletion of AKR7A5 from liver extracts shows that it is one of the major liver 2-CBA reductases but that it is not the main SSA reductase in this tissue.

Key words: Aldo-keto reductase; Succinic semialdehyde; Mouse liver; Carbonyl metabolism

1. Introduction

Aldehydes and ketones form the reactive group in many endogenous and exogenous compounds, many of which are toxic, mutagenic or carcinogenic [1]. The ability of mammalian cells to metabolise these compounds depends on the presence of enzymes, including members of the aldo-keto reductase (AKR) family [2], aldehyde dehydrogenases [3], alcohol dehydrogenases [4], carbonyl reductase [5], quinone reductase [6] and glutathione *S*-transferases (GSTs) [7].

Studies on the roles of AKR in carbonyl metabolism have assumed greater prominence in recent years, and this family currently comprises 12 subfamilies (AKR1–AKR12) [8,9]. Mouse liver AKRs represent a group of enzymes that contribute to the metabolism of exogenous and endogenous compounds. Enzymes present in adult mouse liver that have been cloned and characterised to date include AKR1C6 (17-β-hydroxysteroid dehydrogenase) [10], AKR1C12 and AKR1C13 [11], and AKR1E1 [12]. However, no members of the major aldehyde reductase AKR1A subfamily have been identified in mouse liver to date. The distantly related AKR7 family includes the rat liver aflatoxin B_1 aldehyde reductase or AFAR (AKR7A1), a second rat enzyme AKR7A4 [13,14] and two human homologues AKR7A2 [15] and AKR7A3 [16].

AKR7A1 was originally discovered as an inducible aflatoxin B_1 dialdehyde reductase present in the livers of rats fed on diets containing the synthetic antioxidant ethoxyquin [17,18]. Subsequent studies revealed that AKR7A1 is also induced by a wide range of xenobiotics including butylated hydroxyanisole, coumarin, oltipraz and benzyl isothiocyanate [19]. It is thought the gene is transcriptionally activated via an antioxidant responsive element [20]. Following the characterisation of this inducible rat AKR, another related reductase has been found in rat (AKR7A4) [13] and two related human reductases (AKR7A2 and AKR7A3) [15,16] have also been isolated. Enzyme studies of these rat and human AKR7 enzymes have shown that they are capable of reducing aflatoxin B_1 aldehyde [15,16,21]. In addition, rat AKR7A1, human AKR7A2 and human AKR7A3 have all been shown to have substantial activity towards succinic semialdehyde (SSA), suggesting that this compound, which is derived from γ-aminobutyrate (GABA), may represent an important physiological substrate for the AKR7A enzyme family [13,15,16,22]. Both rat AKR7A4 and human AKR7A2 proteins have been identified in brain, suggesting a potential role in the biosynthesis of γ-hydroxybutyrate (GHB), an important neurotransmitter, from SSA [23]. In addition to exhibiting SSA reductase activity, AKR7A family members are also able to metabolise 2-carboxybenzaldehyde (2-CBA), a compound that is structurally similar to SSA. Very few other AKRs can reduce 2-CBA, making this a relatively specific substrate for AKR7A family members. Crystallisation of AKR7A1 has allowed the structure of this dimeric AKR to be determined, and has provided a structural basis for the enzyme's ability to reduce 4-carbon acid aldehydes such as 2-CBA and SSA [24].

A precise physiological function based on substrate specificity or tissue distribution alone has been difficult to determine for any of the currently known AKR7A enzymes. At present it is not clear whether the rat AKR7A1 is the functional homologue of either human AKR7A2 or AKR7A3 and there is no available evidence to suggest that either of the human enzymes is inducible. Because of the potential usefulness of mouse as a model for investigating in vivo carbonyl metabolism and detoxication, the cloning, expression, and characterisation of a hitherto unrecognised AKR7A enzyme in the mouse is described, which it is hoped will lead to future in vivo functional analysis of the AKR7A gene family.

*Corresponding author. Fax: (44)-141-553 4124.
E-mail address: elizabeth.ellis@strath.ac.uk (E. Ellis).

Abbreviations: AKR, aldo-keto reductase; SSA, succinic semialdehyde; GHB, γ-hydroxybutyrate; 2-CBA, 2-carboxybenzaldehyde; 4-NBA, 4-nitrobenzaldehyde; GST, glutathione *S*-transferase; 9,10-PQ, 9,10-phenanthrenequinone; NQO1, NAD(P)H:quinone oxidoreductase; GABA, γ-aminobutyrate

0014-5793/02/$22.00 © 2002 Published by Elsevier Science B.V. on behalf of the Federation of European Biochemical Societies.
PII: S0014-5793(02)02982-4

2. Materials and methods

2.1. Cloning of mouse AKR7A5 cDNA

Comparison between rat AKR7A1 nucleotide sequences and other cDNAs was carried out by BLAST searching [25] against the GenBank database. A partial mouse AKR7A5 complementary DNA was initially amplified by RT-PCR using total mouse liver RNA as a source and oligos designed to the expressed sequence tag (EST) sequences AA111743 and W50781 (MA3 – 5′-CCG.GAATTC.GCGTCGCATGGATGCGAGTGCTGCTAGCG-3′ and MA2 – 5′-CGG.GGTACC.GGACACTCGTGGGCGACC-3′). This truncated cDNA was cloned into pT7Blue3 to give pAH10 and was used to probe Northern blots. To determine the full-length cDNA sequence, SMART (switching mechanism at 5′ end of RNA transcript) RACE (rapid amplification of cDNA ends) PCR was performed. Two gene specific primers for the 3′ and 5′ RACE (GSP1 – 5′-CGTCCGGTCCCAGTTAGAGACGTCTCTG-3′; GSP2 – 5′-CCAAAGAAGCGGCCCACGGGTTGTTTCC-3′) were used in conjunction with primers specific for oligonucleotides that had been incorporated into the 5′ and 3′ ends of cDNA derived from mouse liver mRNA. The full-length cDNA was then amplified from reverse-transcribed mouse liver RNA, using two oligonucleotides, one of which (mAFARFOR 5′-CGCTCCGGGACTTCGGTCGGGC-3′) was designed to a third EST (accession no. AI893701) and the other (mAFARRev 5′-TGCTTTATTCAGACAGGA-3′) was designed to the 3′ end from the sequence derived from the SMART RACE PCR. The sequence of the amplicon was verified and it was then used as template for a second round of PCR with primers: mAFAR1 5′-CCGGAATTCCAT.ATGTCCCGGCCTCCGCCACCCCGC-3′ (forward) and mAFAR2 5′-CGGCTCGAG.CTATCTGAAGTAGGTTGGGACA-3′ (reverse) which included 5′ *Eco*RI and *Nde*I sites and a 3′ *Xho*I site. This full-length mouse AKR7 cDNA was blunt cloned into the multiple cloning site of pT7Blue3 (Novagen) between the *Eco*RI sites resulting in pAH11. The DNA insert in pAH11 was sequenced to verify fidelity of amplification using dye terminators and Amplitaq FS DNA polymerase and separated on an ABI (Applied Biosystems) 373A automated sequencer. Multiple sequence alignments of AKR7A family members were carried out using Clustal-X [26].

2.2. Bacterial expression and isolation of recombinant AKR7A enzyme

The coding region for mouse AKR7A5 was excised from pAH11 by digestion with *Nde*I and *Xho*I, and ligated into the *Nde*I and *Xho*I sites of pET15b expression vector. The resulting expression construct pAH12 was used to transform *Escherichia coli* BL21 pLysS. Expression of recombinant His-tagged AKR7A5 protein was induced for 1.5 h at 37°C by the addition of 0.5 mM isopropyl β-D-thiogalactoside to mid-exponential phase transformed BL21 pLysS cells. Cells were harvested by centrifugation, frozen at −70°C, and lysed using a sonicator in buffer A (20 mM sodium phosphate, 500 mM NaCl pH 7.4). Lysates were filtered through a 0.45 μm Whatman polysulphone disc, and loaded onto a 5 ml HiTrap Chelating affinity column (Pharmacia Biosystems Ltd., Milton Keynes, Herts, UK), pre-equilibrated with buffer A. After washing the column, recombinant polyhistidine-tagged protein was recovered by elution with 200 mM imidazole in buffer A. The eluted recombinant protein was then passed through a G25 gel filtration system column, equilibrated with 20 mM sodium phosphate buffer (pH 6.6) to remove the imidazole and salt. 10% (v/v) glycerol was added and purified enzyme to be stored at −70°C. Removal of the His-tag was achieved using human thrombin (Sigma, Poole, UK). Molecular weight estimation was performed using a DYNA-PRO 801 dynamic light scattering/molecular sizing instrument (Protein Solutions, Buckingham, UK).

2.3. Antibodies to AKR7A5

Purified mouse AKR7A5 (approximately 100 μg in 1 ml 10 mM sodium phosphate buffer; pH 7) was emulsified with an equal volume of Freund's complete adjuvant and injected subcutaneously at four separate sites on the back of two female New Zealand White rabbits. After 14 days each rabbit was re-inoculated with 100 μg of the original immunogen in incomplete Freund's adjuvant and this was followed by a final inoculation 10 days later, this time with 100 μg of immunogen in 0.9% saline. After a further 10 days the animals were killed and bled. The serum obtained was stored at −20°C, in the presence of 0.1% sodium azide until required.

2.4. Protein and enzyme assays

Protein concentrations were measured using the method of Bradford [27] and standardised using bovine serum albumin, using a kit from Bio-Rad Laboratories Ltd. (Hemel Hempstead, UK). Aldehydes and ketone substrates were obtained from Sigma Chemical Co. (Poole, Dorset, UK) or from Aldrich Chemical Co. (Gillingham, Dorset, UK). Aflatoxin B_1 dialdehyde was prepared using previously described methods, which allow the formation of the dialdehyde from the dihydrodiol [28]. Aldehyde- and ketone-reducing activity was routinely measured with a Beckman DU650 UV single-beam recording spectrophotometer by following the initial rate of oxidation of NADPH at 340 nm ($\in = 6270\ M^{-1}\ cm^{-1}$) as described previously [22]. Apparent K_m values for mouse AKR7A5 were determined by measuring the initial reaction rate over a range of substrate concentrations and were calculated using Ultrafit curve-fitting software (Biosoft, Cambridge, UK) using the Marquardt algorithm.

2.5. Protein gels and Western blots

SDS–PAGE was performed in 12% polyacrylamide resolving gels with the buffer system described by Laemmli [29]. For Western blotting, electrophoretic transfer of polypeptides from SDS–PAGE gels to nitrocellulose membranes was carried out using a Bio-Rad minigel apparatus. Protein binding sites on membranes were blocked overnight in TBST (20 mM Tris–HCl/150 mM NaCl/0.01% (v/v) Tween) which contained 10% (w/v) skimmed milk. The blots were then incubated for 1 h at room temperature with antisera against AKR7A5 or NAD(P)H:quinone oxidoreductase (NQO1) (at 1:2000 dilution in TBST). After washing, horseradish peroxidase-conjugated secondary antibody (goat anti-rabbit IgG, at 1:3000 dilution) in TBST was added. The antibody complexes were detected using enhanced chemiluminescence (ECL; Amersham).

2.6. Animals and preparation of tissue extracts

Eight week old male CD-1 mice were fed a basic diet of powdered food with arachis oil, or the basic diet/arachis oil plus 0.5% (w/w) ethoxyquin, butylated hydroxyanisole, coumarin or benzyl isothiocyanate for 7 days immediately before sacrifice. Upon removal, the organs from the CD-1 mice were snap-frozen and stored at −70°C until use. To prepare the cell extracts approximately 100 mg of each tissue was taken and homogenised in 20 mM $NaPO_4$ buffer (pH 7.0). After centrifugation to remove cell debris, supernatant fractions were stored at −80°C.

AKR7A5 was immunodepleted from total liver extracts as follows: a 100 μl aliquot of preswollen protein A-Sepharose beads (approximately 50% slurry) was added to 200 μl of antisera (either against AKR7A5 or LDH). After incubation at 4°C for 1 h, portions of extracts containing equivalent amounts of AKR7A5 (as estimated from quantitative Western blots) diluted into 200 μl of ice-cold 10 mM sodium phosphate buffer (pH 8.0) were added to each of the protein–antibody mixtures; after incubation at 4°C for 2 h, the beads were removed by centrifugation. Complete removal of AKR7A5 from the extracts was verified by Western blot analysis of the supernatants (data not shown). The resulting AKR7A5- and LDH-depleted supernatants were then assayed for carbonyl-reducing activity.

3. Results and discussion

3.1. Identification and cloning of mouse AKR7A5

The rat AKR7A1 sequence was used to carry out a BLAST search against the GenBank database. This identified several mouse ESTs whose predicted gene products showed extensive similarity to AKR7A1 at the amino acid level. Two of these sequences (AA111743 and AI893701) were derived from adult kidney cDNA whereas the third was embryonic in origin. These ESTs were identical in their overlapping regions, suggesting that they were derived from the same gene (Fig. 1).

SMART RACE PCR was used in an attempt to determine whether the sequence represented the full-length mouse AKR7A-related sequence. Sequencing of these amplicons revealed additional sequence at the 3′ end, including the polyA

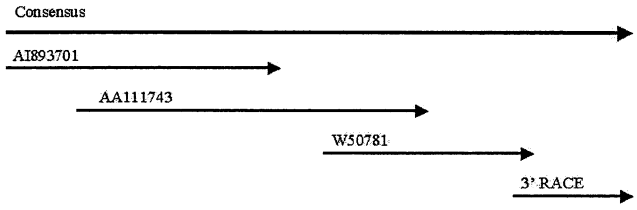

Fig. 1. Alignment of mouse EST showing similarity to rat AKR7A1 cDNA. Three ESTs were identified by using the AKR7A1 cDNA sequence to perform BLAST search of the GenBank database. Additional 3′ sequence was derived from 3′ RACE of mouse liver mRNA. The full-length sequence has been deposited in the EMBL database.

tail. However, no additional sequence could be determined at the 5′ end beyond that which was present in EST AI893701.

To confirm that this sequence represents a bone fide cDNA that is expressed in mouse liver, RT-PCR was performed from mouse liver total RNA using primers to the 5′ and 3′ ends of the proposed sequence. A PCR product of 1.01 kb was isolated, cloned and the full-length sequence was confirmed by DNA sequencing. The consensus sequence resulted in an open reading frame of 1017 bp, which would translate to a polypeptide of 338 residues with an estimated molecular mass of 37 662 Da. Comparison of this putative mouse AKR7A and other already identified AKR7A enzymes (Fig. 2) showed these proteins are highly related. At the amino acid level the putative mouse AKR7A is 78% identical to the ethoxyquin-inducible aflatoxin dialdehyde reductase (AFAR; AKR7A1) from rat liver and 88% identical to both human AKR7A2 and AKR7A3. From this sequence similarity alone it might be expected to perform a similar role to one or more of these enzymes. In common with its close relatives, it shares less than

```
                                                                  +    +
AKR7A4          MSRSPAPRAVSGAPLRPGTVLGTMEMGRRMDASASAATVRAFLERGLNELDTAFMYCDGQ
AKR7A5          MSRPPPPRAASGAPLRPATVLGTMEMGRRMDASASAASVRAFLERGHSELDTAFMYCDGQ
AKR7A2          MSRPPPPRVAS--------VLGTMEMGRRMDAPASAAAVRAFLERGHTELDTAFMYSDGQ
AKR7A3          MSRQLS-RARP------ATVLGAMEMGRRMDAPTSAAVTRAFLERGHTEIDTAFVYSDGQ
AKR7A1          MSQARP-----------ATVLGAMEMGRRMDVTSSSASVRAFLQRGHTEIDTAFVYANGQ
                **:  .             ***:********..:*:* .****:** .*:****:*.:**

                                    +                                    +
AKR7A4          SESILGSLGLGLGSGDCTVKIATKANPWDGKSLKPDSVRSQLETSLKRLQCPRVDLFYLH
AKR7A5          SENILGGLGLGLGSGDCTVKIATKANPWEGKSLKPDSVRSQLETSLKRLQCPRVDLFYLH
AKR7A2          SETILGGLGLGLGGGDCRVKIATKANPWDGKSLKPDSVRSQLETSLKRLQCPQVDLFYLH
AKR7A3          SETILGGLGLRLGGSDCRVKIDTKAIPLFGNSLKPDSLRFQLETSLKRLQCPRVDLFYLH
AKR7A1          SETILGDLGLGLGRSGCKVKIATKAAPMFGKTLKPADVRFQLETSLKRLQCPRVDLFYLH
                **.***.*** ** ..* *** *** *  *::*** .:* ************:*******


AKR7A4          APDHGTPIVETLQACQQLHQEGKFVELGLSNYASWEVAEIYTLCKSNGWILPTVYQGMYN
AKR7A5          APDHSTPVEETLRACHQLHQEGKFVELGLSNYASWEVAEICTLCKSNGWILPTVYQGMYN
AKR7A2          TPDHGTPVEETLHACQRLHQEGKFVELGLSNYASWEVAEICTLCKSNGWILPTVYQGMYN
AKR7A3          MPDHSTPVEETLRACHQLHQEGKFMELGLSNYAAWEVAEICTLCKSNGWILPTVYQGMYN
AKR7A1          FPDHGTPIEETLQACHHVHQEGKFVELGLSNYVSWEVAEICTLCKKNGWIMPTVYQGMYN
                 ***.**: ***:**:::******:*******.:****** ****.****:*********


AKR7A4          ATTRQVETELLPCLRYFGLRFYAYNPLAGGLLTGKYRYEDKDGKQPEGRFFGNSWSETYR
AKR7A5          ATTRQVEAELLPCLRHFGLRFYAYNPLAGGLLTGKYKYEDKDGKQPVGRFFGNNWAETYR
AKR7A2          ATTRQVETELFPCLRHFGLRFYAYNPLAGGLLTGKYKYEDKDGKQPVGRFFGNSWAETYR
AKR7A3          AITRQVETELFPCLRHFGLRFYAFNPLAGGLLTGKYKYEDKDGKQPVGRFFGNTWAEMYR
AKR7A1          AITRQVETELFPCLRHFGLRFYAFNPLAGGLLTGRYKYQDKDGKNPESRFFGNPFSQLYM
                * *****:**:****:*******:**********:*:*:*****:* .***** ::: *


AKR7A4          NRFWKEHHFEAIALVEKALKTTYGTSAPSMTSAALRWMYHHSQLQGTRGDAVILGMSSLE
AKR7A5          NRFWKEHHFEAIALVEKALQTTYGTNAPRMTSAALRWMYHHSQLQGTRGDAVILGMSSLE
AKR7A2          NRFWKEHHFEAIALVEKALQAAYGASAPSVTSAALRWMYHHSQLQGAHGDAVILGMSSLE
AKR7A3          NRYWKEHHFEGIALVEKALQAAYGASAPSMTSATLRWMYHHSQLQGAHGDAVILGMSSLE
AKR7A1          DRYWKEEHFNGIALVEKALKTTYGPTAPSMISAAVRWMYHHSQLKGTQGDAVILGMSSLE
                :*:***.**:.********:::**..** : **::*********:*::************


AKR7A4          QLEQNLAATEEGPLEPAVVEAFNQAWNVVAHECPNYFR
AKR7A5          QLEQNLAATEEGPLEPAVVEAFDQAWNMVAHECPNYFR
AKR7A2          QLEQNLAATEEGPLEPAVVDAFNQAWHLVAHECPNYFR
AKR7A3          QLEQNLAAAEEGPLEPAVVDAFNQAWHLVAHECPNYFR
AKR7A1          QLEQNLALVEEGPLEPAVVDAFDQAWNLVAHECPNYFR
                ******* .**********:**:***::**********
```

Fig. 2. Multiple sequence alignment of full-length mouse AKR7A5 with rat and human AKR7A sequences. Clustal-X multiple sequence alignment between the amino acid sequences of AKR7A5 and other AKR7A. *, identical amino acids; : and ., conserved amino acids; +, amino acids corresponding to the catalytic tetrad.

20% identity with other mouse AKRs in the major AKR1 family, and also shows some similarity in structure and sequence to the voltage-gated *Shaker*-related K^+ channel β-subunit AKR6 family. The four amino acids forming the catalytic tetrad shown to be involved in catalysis in other AKRs [30] are conserved in mouse AKR7A (Tyr-56, His-130, Lys-84 and Asp-51), suggesting that the mouse sequence is likely to encode an active enzyme.

3.2. Catalytic properties of mouse AKR7A5

To determine whether the mouse AKR7A-related protein was catalytically active, the coding region was cloned into a bacterial expression vector, and the protein purified as described previously for rat AKR7A1 [18]. Removal of the N-terminal His-tag using thrombin resulted in a protein which co-migrated with an AKR7-related protein present in mouse liver extracts (Fig. 3A), indicating that it represents the full-length protein that is expressed in liver. Dynamic light scattering analysis showed the purified protein to be monodispersed, with a hydrodynamic radius of 3.8 nm, giving it an estimated molecular weight of 77 kDa. This means that the purified recombinant protein is a dimer, a feature which it shares with rat AKR7A1 and AKR7A4 [13,24].

Enzyme assays were performed which showed that the purified recombinant mouse protein was able to reduce the mod-

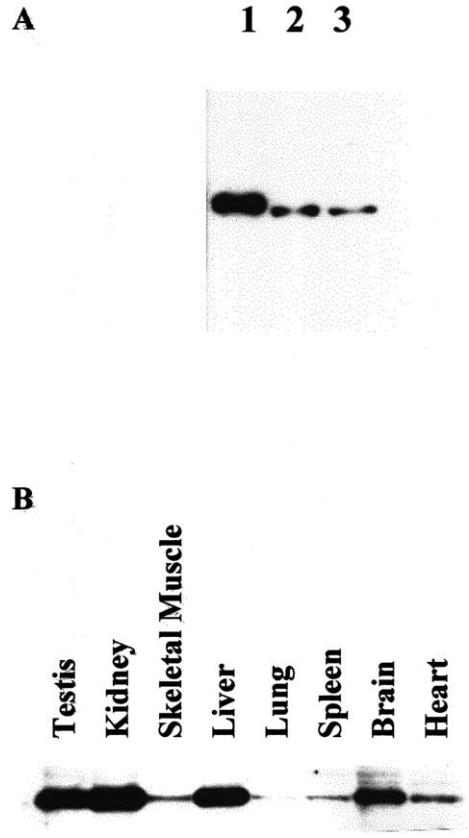

Fig. 3. Detection of AKR7A5 in mouse tissues. Detection of recombinant AKR7A5 and an AKR7A5-related band in mouse tissues was carried out by separating purified protein and tissue extracts by SDS–PAGE and subjecting to Western blotting. The membranes were probed with antisera raised to AKR7A5 and detected using ECL. A: 1, Recombinant AKR7A5; 2, recombinant AKR7A5 after cleavage of the His-tag with thrombin; 3, 10 μg mouse liver extract. B: 10 μg extract of the mouse tissues indicated.

el substrate 4-nitrobenzaldehyde (4-NBA). It was therefore given the name AKR7A5 as it represents the fifth active member of the subfamily to be characterised. Like the rat and human AKR7A enzymes, the mouse enzyme can use both NADH and NADPH as cofactor (Table 1). Using 4-NBA as a substrate, and NADPH as a cofactor, the optimum pH for the mouse AKR7A5 was determined and found to be pH 6.6, but the enzyme can function over a broad range (pH 5.0–9.0). AKR7A5 also demonstrates a broad range of substrate specificities for aldehydes and diketones, including drugs, toxic aldehydes, and metabolites.

The apparent Michaelis constants of the recombinant mouse AKR7A5 for some relevant substrates were determined (Table 1). Mouse AKR7A5 can reduce the dialdehyde form of AFB_1-dihydrodiol (pH 8.5), although it has a lower affinity (K_m 90 μM) compared with that determined previously for the rat and human enzymes (9 μM) [16,21]. This is particularly salient because it had been thought that an aflatoxin-metabolising aldehyde reductase would not be important for detoxication of this compound in mouse because of the high constitutive presence of a specific alpha class GST in this species. This GST is able to conjugate the aflatoxin 8,9-epoxide and was thought to be responsible for conferring the high level of resistance to aflatoxin B_1 seen in mouse [31]. A similar GST is inducible in rat [32]. In humans, the AKR7A enzymes are considered to assume greater importance [21]. The catalytic efficiency that we observe suggests that AKR7A5 may also make a contribution to aflatoxin resistance in the mouse.

AKR7A5 is also capable of reducing *trans, trans*-muconaldehyde which is a toxic metabolite of benzene and has been linked to the occurrence of leukaemia. The endogenous monoamine oxidase inhibitor isatin has been shown previously to be a good substrate for human AKR7A2 [15], and likewise, it is also a good substrate for mouse AKR7A5 with a K_m of 109 μM. However, mouse AKR7A5 has very weak affinity for some dicarbonyls such as diacetyl (K_m 58 mM), which marks it as clearly different from rat AKR7A1. The affinity of the enzyme for NADH is significantly lower than that observed for NADPH (Table 1) when using 4-NBA as substrate.

The kinetic constants of the mouse, rat and human AKR7A enzymes were compared for some model AKR substrates: SSA, 9,10-phenanthrenequinone (9,10-PQ), 4-NBA and also 2-CBA, which has been identified as a relatively specific substrate for AKR7A enzymes (Table 2). Mouse AKR7A5 had a similar affinity for 4-NBA ($K_m = 870$ μM) as rat AKR7A1 ($K_m = 520$ μM), whereas human AKR7A2 had significantly lower affinity ($K_m = 6630$ μM). All of the AKR7A enzymes tested reduced the bulky hydrophobic dicarbonyl compound 9,10-PQ, but the mouse and human enzymes have higher affinity and catalytic activity. SSA, which has been shown previously to be reduced by human AKR7A2 [15], is also reduced efficiently by mouse AKR7A5, whereas rat AKR7A1 has a much lower affinity and turn over rate than the mouse or human enzyme.

Table 2
Comparison of catalytic efficiency of recombinant mouse AKR7A5, rat AKR7A1 and human AKR7A2

	K_{cat}/K_m (min^{-1} M^{-1})		
	Mouse AKR7A5	Rat AKR7A1	Human AKR7A2
4-NBA	5.34×10^4	9.55×10^4	1.1×10^4
9,10-PQ	7.69×10^6	4.13×10^6	1.48×10^7
2-CBA	4.86×10^6	1.41×10^7	1.14×10^7
SSA	4.00×10^6	1.06×10^6	3.02×10^6
2-NBA	1.62×10^5	1.4×10^5	6.23×10^4

The activities of AKR7A5, AKR7A1 and AKR7A2 towards carbonyl-containing compounds were determined at 25°C as described in Section 2 using NADPH as cofactor. Apparent K_m and K_{cat} values were estimated from the initial velocities measured over a range of substrate concentrations using the Ultrafit curve-fitting programme.

3.3. Tissue distribution of mouse AKR7A5

Antibodies raised against mouse AKR7A5 were used to probe Western blots of various mouse tissue protein extracts (Fig. 3B). Mouse AKR7A5 antibodies reacted with a protein band in most tissues tested; however, levels are highest in liver, kidney, testis and brain, and lower levels were found in the heart, spleen, and skeletal muscle. This pattern of expression differs from rat AKR7A1, as the rat protein is only detectable at low levels in the livers of control rats and is present additionally only in testis, kidney and small intestine [18]. The tissue distribution of AKR7A5 is more similar to that seen for the human AKR7A2 protein which is expressed in most tissues and is detected at high levels in liver, kidney,

Table 1
Apparent kinetic constants for mouse AKR7A5 for aldehyde and diketone substrates

Substrate	Mouse AKR7A5		
	K_m (μM)	K_{cat} (min^{-1})	K_{cat}/K_m (min^{-1} M^{-1})
4-NBA	870 ± 500	46 ± 6	5.34×10^4
9,10-PQ	8.0 ± 4.0	62 ± 6	7.69×10^6
2-CBA	16 ± 3	78 ± 17	4.86×10^6
SSA	20 ± 10	80 ± 12	4.02×10^6
AFB_1-dihydrodiol (pH 8.5)	90 ± 30	34 ± 7	3.77×10^5
Isatin	109 ± 26	54 ± 3	4.99×10^5
2-NBA	460 ± 140	75 ± 11	1.63×10^5
Methyl glyoxal	3 980 ± 940	47 ± 3	1.18×10^4
Camphorquinone	4 990 ± 490	66 ± 3	1.32×10^4
Trans, trans-muconaldehyde	7 190 ± 5 990	94 ± 41	1.31×10^4
Diacetyl	58 420 ± 16 410	114 ± 1	1.96×10^3
NADPH	1.62 ± 0.01	26 ± 3	1.58×10^7
NADH	1 470 ± 23	115 ± 101	7.86×10^4

The activity of AKR7A5 towards carbonyl-containing compounds was determined at 25°C as described in Section 2 using NADPH as cofactor. Apparent K_m and K_{cat} values were estimated from the initial velocities measured over a range of substrate concentrations using the Ultrafit curve-fitting programme. The values shown represent mean ± S.E.M. The K_m and K_{cat} for NADPH and NADH were estimated using 4-NBA as substrate.

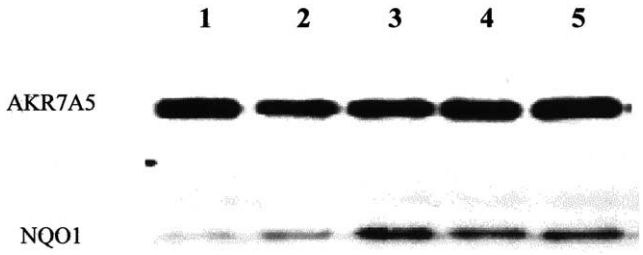

Fig. 4. Induction of mouse liver enzymes by chemoprotectors. Portions (10 μg) of hepatic extract from control male mice and from male mice that had been fed ethoxyquin, *tert*-butyl hydroquinone, coumarin, indole-3-carbinol or benzyl isothiocyanate were separated by electrophoresis on a single SDS–PAGE gel. After blotting, the nitrocellulose membrane was probed with antisera raised to AKR7A5 or NQO1. Cross reacting polypeptides were visualised by ECL. 1, Control diet; 2, coumarin; 3, ethoxyquin; 4, butylated hydroxyanisole; 5, benzyl isothiocyanate.

testis and, importantly, brain [33]. The narrow tissue distribution of the rat enzyme suggested that it has a specialised tissue specific role, possibly in detoxication. By contrast, the more widespread rat AKR7A4 and human AKR7A2 tissue distribution suggests that these enzymes may perform a 'housekeeping' role, possibly in metabolism [13,15]. Overall, the mouse enzyme distribution seems to fit more closely with the latter two enzymes, suggesting that it too performs a house-keeping role.

3.4. Induction of mouse liver enzymes by chemoprotectors

An unusual feature of the rat AKR7A1 is that its expression in liver is inducible by a variety of chemopreventive compounds, including synthetic antioxidants such as ethoxyquin, butylated hydroxyanisole and oltipraz [34]. It is therefore considered to be a key detoxication enzyme that is part of an adaptive stress response to chemical and oxidative stress [20]. In contrast, rat AKR7A4 is found to be constitutively expressed in the liver [13]. To determine whether AKR7A5 was inducible, mice were fed on diets containing ethoxyquin, butylated hydroxyanisole, coumarin, and benzyl isothiocyanate for 7 days and the livers examined for increased expression of AKR7A5 and NQO1, an enzyme previously shown to be inducible by these compounds. Fig. 4 shows that although the treatments lead to the induction of NQO1, there is no increase in the levels of AKR7A5. The lack of inducibility of AKR7A5 suggests that AKR7A5 is assuming a role similar to the constitutive rat AKR7A4. It is possible that the inducibility of AKR7A1 is a feature unique to the rat. Neither of the human enzymes AKR7A2 and AKR7A3 has been shown to be inducible in the liver, though there does appear to be some interindividual variation in expression levels and activities [21,33].

3.5. Contribution of mouse AKR7A5 to liver carbonyl-reducing activity

A low K_m for SSA suggested that the mouse AKR7A5 could function as a SSA reductase in vivo, as has been proposed for human AKR7A2 [15]. To assess the role of mouse AKR7A5 in the metabolism of SSA in liver, we depleted liver extracts using antibodies raised to AKR7A5 (Fig. 5). This showed that SSA reductase activity in mouse liver does not decrease when mouse AKR7A5 is removed, which indicates that it is not the primary SSA reductase enzyme in mouse liver. In many tissues, SSA is produced from GABA by GABA-transaminase and is metabolised by SSA dehydrogenase to succinic acid. However, SSA can also be reduced by SSA reductase in some tissues to GHB, particularly where SSA dehydrogenase is not ubiquitously expressed. GABA-transaminase is widely distributed in non-neural tissues, including liver, kidney and testis whereas SSA dehydrogenase is absent from some of those tissues such as the testis. A role for AKR7A2 in the reduction of SSA has been supported by the purification of AKR7A2 from human brain as a major SSA reductase [23]. Similarly, AKR7A-related proteins are expressed in rat brain [13,35]. However, it has been demonstrated that AKR7A2 does not constitute the major SSA reductase in human liver [15], as the major peak of SSA reductase activity does not copurify with AKR7A2. A similar observation was seen in rat liver where neither of the two rat enzymes AKR7A1 or AKR7A4 was present in the major SSA reductase peak [13]. Our results suggest that AKR7A5 is not the major SSA reductase in liver, which is concordant with it paralleling the function of human AKR7A2. Presumably another AKR such as an aldehyde reductase of the AKR1 family contributes the majority of SSA reductase activity in the liver. Further work is required to establish whether AKR7A5 is a major SSA reductase in mouse brain, particularly if other AKRs are not present in this tissue.

Immunodepletion experiments did, however, reveal that there is a significant decrease (40%) in hepatic 2-CBA reductase activity following removal of AKR7A5 from the extracts. 2-CBA is a carbonyl compound that is of interest to the pharmaceutical industry because it is used to mask drugs and enhance their delivery to target sites [36,37]. It has been previously reported that AKR7A2 is the principal 2-CBA reductase in human liver [15], and our data suggest that this role may also be shared by AKR7A5 in mouse liver. Immunodepleted extracts also showed that AKR7A5 is responsible for approximately 15% of the total hepatic 4-NBA reductase activity (Fig. 5), but did not show any decrease in 9,10-PQ reductase activity, suggesting that it is not the major liver enzyme responsible for the reduction of this compound (Fig. 5).

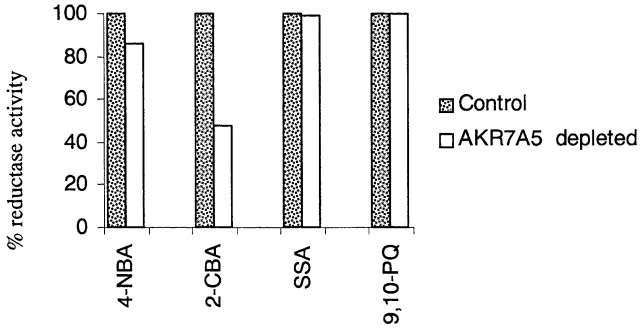

Fig. 5. Carbonyl-reducing activities in hepatic cytosols immunodepleted for AKR7A5. Extracts from the livers of three mice that had been fed either control diet or control diet plus ethoxyquin were incubated with antisera raised against AKR7A5 (open bar) or LDH (speckled bar) (as a control) and protein A-Sepharose beads. After removal of the beads by centrifugation, the remaining activities in the immunodepleted samples were assayed for the substrates indicated. Data represent the mean of three experiments ($n = 3$).

4. Conclusions

The data we present point to the mouse AKR7A5 being the functional orthologue of human AKR7A2 and rat AKR7A4. This conclusion is based on the fact that it shares similar enzyme kinetic properties, tissue distribution pattern and does not appear to be inducible. In addition, we have shown that it, like the human AKR7A2 and rat AKR7A4 enzymes, is not the major SSA reductase in liver, but that it is likely to contribute to 2-CBA reduction in that tissue. It may also play a role in aflatoxin B_1 dialdehyde reduction in mouse liver, thus contributing to constitutive resistance to the aflatoxin. A role for AKR7A5 as a SSA reductase in brain remains to be established.

The characterisation of the enzyme described here will pave the way for its function in vivo to be investigated through the generation of a mouse line in which the AKR7A5 gene has been knocked out. This will enable future investigations into its role in detoxication and drug metabolism, as well as its potential role in the metabolism of aldehydes in the brain.

Acknowledgements: We are grateful to Prof. Iain Hunter for use of the spectrophotometer and to Dr. Adrian Lapthorn for use of the dynamic light scattering machine. We thank Prof. Gisela Witz for supplying *trans, trans*-muconaldehyde. A.H. was supported by a Bell College Postgraduate Studentship.

References

[1] Sladek, N., Manthey, C., Maki, P., Zhang, Z. and Landkamer, G. (1989) Drug Metab. Rev. 20, 697–720.
[2] Penning, T.M. (1993) Chem. Biol. Interact. 89, 1–34.
[3] Wang, X.P., Sheikh, S., Saigal, D., Robinson, L. and Weiner, H. (1996) J. Biol. Chem. 271, 31172–31178.
[4] Leiber, C.S. (1994) J. Toxicol. Clin. Toxicol. 32, 631–681.
[5] Maser, E. (1995) Biochem. Pharmacol. 49, 421–440.
[6] Li, R., Bianchet, M.A., Talalay, P. and Amzel, L.M. (1995) Proc. Natl. Acad. Sci. USA 92, 8846–8850.
[7] Hayes, J.D. and Pulford, D.J. (1995) Crit. Rev. Biochem. Mol. Biol. 30, 445–600.
[8] Jez, J. and Penning, T.M. (2001) Chem. Biol. Interact. 130–132, 499–525.
[9] Jez, J., Flynn, T. and Penning, T. (1997) Biochem. Pharmacol. 54, 639–647.
[10] Deyashiki, Y., Ohshima, K., Nakanishi, M., Sato, K., Matsuura, K. and Hara, A. (1995) J. Biol. Chem. 270, 10461–10467.
[11] Ikeda, S., Okuda-Ashitaka, E., Masu, Y., Suzuki, T., Watanabe, K., Nakao, M., Shingu, K. and Ito, S. (1999) FEBS Lett. 459, 433–437.
[12] Bohren, K., Barski, O. and Gabbay, K. (1996) in: Enzymology and Molecular Biology of Carbonyl Metabolism 6 (Weiner, H., Ed.), Plenum Press, New York.
[13] Kelly, V.P., Ireland, L.S., Ellis, E.M. and Hayes, J.D. (2000) Biochem. J. 348, 389–400.
[14] Nishi, N., Shoji, H., Miyanaka, H. and Nakamura, T. (2000) Endocrinology 141, 3194–3199.
[15] Ireland, L., Harrison, D., Neal, G. and Hayes, J. (1998) Biochem. J. 332, 21–34.
[16] Knight, L.P., Primiano, T., Groopman, J.D., Kensler, T.W. and Sutter, T.R. (1999) Carcinogenesis 20, 1215–1223.
[17] Hayes, J., Judah, D. and Neal, G. (1993) Cancer Res. 53, 3887–3894.
[18] Ellis, E., Judah, D., Neal, G. and Hayes, J. (1993) Proc. Natl. Acad. Sci. USA 90, 10350–10354.
[19] Ellis, E., Judah, D., Neal, G., OConnor, T. and Hayes, J. (1996) Cancer Res. 56, 2758–2766.
[20] Hayes, J., Ellis, E., Neal, G., Harrison, D. and Manson, M. (1999) Biochem. Soc. Symp. 64, 141–168.
[21] Guengerich, F.P., Cai, H., McMahon, M., Hayes, J.D., Sutter, T.R., Groopman, J.D., Deng, Z. and Harris, T.M. (2001) Chem. Res. Toxicol. 14, 727–737.
[22] Ellis, E. and Hayes, J. (1995) Biochem. J. 312, 535–541.
[23] Schaller, M., Schaffhauser, M., Sans, N. and Wermuth, B. (1999) Eur. J. Biochem. 265, 1056–1060.
[24] Kozma, E., Brown, E., Ellis, E.M. and Lapthorn, A. (2002) J. Biol. Chem. 277, 16285–16293.
[25] Altschul, S.F., Gish, W., Miller, W., Myers, E.W. and Lipman, D.J. (1990) J. Mol. Biol. 215, 403–410.
[26] Jeanmougin, F., Thompson, J.D., Gouy, M., Higgins, D.G. and Gibson, T.J. (1998) Trends Biochem. Sci. 23, 403–405.
[27] Bradford, M.M. (1976) Anal. Biochem. 72, 248–254.
[28] Johnson, W., Harris, T. and Guengerich, F. (1996) J. Am. Chem. Soc. 118, 8213–8220.
[29] Laemmli, U.K. (1970) Nature (London) 227, 248–254.
[30] Jez, J., Bennett, M., Schlegel, B., Lewis, M. and Penning, T. (1997) Biochem. J. 326, 625–636.
[31] Hayes, J.D., Judah, D.J., Neal, G.E. and Nguyen, T. (1992) Biochem. J. 285, 173–180.
[32] Hayes, J. et al. (1998) Chem.–Biol. Interact. 112, 51–67.
[33] O'Connor, T., Ireland, L., Harrison, D. and Hayes, J. (1999) Biochem. J. 343, 487–504.
[34] Hayes, J., Judah, D., McLellan, L., Kerr, L., Peacock, S. and Neal, G. (1991) Biochem. J. 279, 385–398.
[35] Grant, A., Staffas, L., Mancowiz, L., Kelly, V.P., Manson, M.M., DePierre, J.W., Hayes, J.D. and Ellis, E.M. (2001) Biochem. Pharmacol. 62, 1511–1519.
[36] Jaffe, G., Murphy, J.E. and Robinson, O.P. (1976) Practitioner 216, 455–461.
[37] Moss, J. and Bundgaard, H. (1992) Acta Pharm. Nord. 4, 301–308.